



Distribution and abundance of marine microbes in the Southern Ocean between 30 and 80°E

Paul G. Thomson^{a,e,*}, Andrew T. Davidson^{a,e}, Rick van den Enden^a, Imojen Pearce^{a,e}, Laurent Seuront^{b,c}, James S. Paterson^b, Guy D. Williams^{d,e}

^a Department of the Environment, Water, Heritage and the Arts, Australian Antarctic Division, Channel Highway, Kingston, Tasmania 7050, Australia

^b School of Biological Sciences, Flinders University, GPO Box 2100, Adelaide SA 5001, Australia

^c South Australian Research and Development Institute, Aquatic Sciences, West Beach SA 5022, Australia

^d Institute of Low Temperature Science, Hokkaido University, N19W8, Sapporo 060-0819, Japan

^e Antarctic Climate and Ecosystems Cooperative Research Centre (ACECRC), University of Tasmania, Private Bag 80, Hobart, Tasmania, 7001, Australia

ARTICLE INFO

Article history:

Received 8 October 2008

Accepted 8 October 2008

Available online 24 November 2009

Keywords:

Southern Ocean

Oceanography

Flow cytometry

Marine microbes

Nanophytoplankton

HNF

Bacteria

Lysotracker Green

SYTO 13

SYBR Green

ABSTRACT

Our study, as part of the Baseline Research on Oceanography, Krill and the Environment, West (BROKE-West) survey, emphasised the vital role of sea-ice retreat and upwelling in controlling the distribution, abundance and composition of marine microbial communities in the seasonal ice zone (SIZ). Autofluorescence or stains were used to detect the abundance of nanophytoplankton, heterotrophic nanoflagellates (HNF), virus like particles (VLP) and bacteria by flow cytometry. Correlations among microbial concentrations were determined and cluster analysis was performed to group sites of similar microbial composition and abundance. Distance to sea ice was the primary determinant of nanophytoplankton abundance and nanophytoplankton contributed up to 84% of the phytoplankton carbon biomass where melting sea ice caused shallow summer mixed layer depths. To the north, nanophytoplankton abundance was generally low except adjacent to the Southern Boundary (SB). HNF and bacterial abundance was positively correlated with the abundance of nanophytoplankton. Cluster analysis identified 5 groups of sites over the BROKE-West survey area. Clusters 1–4 grouped sites of different successional maturity of the microbial community along the continuum between bloom formation and senescence. Maturity increased with distance from the sea ice and, in areas of upwelling, with time since the development of phytoplankton blooms. Sites in cluster 5 occurred at the northernmost extreme of the survey area and were typical of communities in high nutrient low chlorophyll (HNLC) waters of the permanent open-ocean zone (POOZ) where phytoplankton growth was matched by mortality and decomposition. Synoptic-scale studies in Antarctic waters are rare but provide vital information about the control of microbial productivity, abundance and distribution in the Southern Ocean. Our study, covering over 40% of the SIZ off East Antarctica, enhances our understanding of the synoptic-scale factors that determine the structure and function of the microbial loop.

Crown Copyright © 2009 Published by Elsevier Ltd. All rights reserved.

1. Introduction

Marine microbes comprise the vast majority of living matter in the ocean. Phytoplankton photosynthesis in the Southern Ocean comprises 5.6–15% of all marine primary production on the earth (Huntley et al., 1991). Sequestration of carbon by phytoplankton supports the wealth of life for which Antarctica is renowned and is one of the worlds' greatest sinks for atmospheric CO₂ (Mikaloff Fletcher et al., 2006). Marine microbes are principal determinants

of the fate of this fixed carbon and understanding energy flow in the marine microbial community is pivotal to developing global carbon budgets (Azam et al., 1991; Legendre et al., 1992; Grossmann and Dieckmann, 1994; Bequevort et al., 2000).

Protozooplankton (2 – 200 μm) play a vital role in the transfer and flux of carbon in the ocean. They are ubiquitous, diverse and can be abundant in Antarctic waters (Garrison, 1991; Becquevort et al., 2000). Their grazing can be the dominant source of phytoplankton and bacterioplankton mortality and can regulate the abundance, size structure and species composition of their prey (Froneman and Perissinotto, 1996; Calbet and Landry, 2004). Nanoprotzoa (2 – 20 μm), including dinoflagellates and HNF, can comprise up to 60% of protozooplankton biomass (Becquevort, 1997; Becquevort et al., 2000; Froneman, 2004) and consume prey of similar size to themselves (Becquevort et al., 1992;

* Corresponding author at: Department of the Environment, Water, Heritage and the Arts, Australian Antarctic Division, Channel Highway, Kingston, Tasmania 7050, Australia. Tel.: +61 3 62323562; fax: +61 3 62323158.

E-mail address: Paul.Thomson@aad.gov.au (P.G. Thomson).

Hansen et al., 1994). HNF grazing impact can exceed that by larger zooplankton when nanophytoplankton are dominant, accounting for >40% of phytoplankton production (Becquevort, 1997; Froneman, 2004; Calbet et al., 2008). Nanoprotozoa are also well known bacterivores and can consume between 27–95% of bacterial production (Safi and Hall, 1999; Christaki et al., 2008; Pearce et al., 2010). As significant grazers of primary and bacterial production, nanoprotozoa are regarded as important trophic intermediates between the larger zooplankton that utilise them as a carbon source and their small sized prey (Becquevort et al., 1992; Jurgen et al., 1996; Froneman and Perissinotto, 1996).

Bacterial metabolism is critical for nutrient remineralisation and element cycling and it is the principal route of carbon flow in aquatic ecosystems, transforming dissolved organic carbon (DOC) into bacterial biomass that supports bacterivores (Azam, 1998). Bacteria can contribute up to 90% of the cellular DNA (Paul et al., 1985; Coffin et al., 1990); 40% of the planktonic carbon (Pomeroy and Wiebe, 1988; Cho and Azam, 1990; Azam, 1998); process up to 80% of the primary production (Larsson and Hagström, 1982; Azam et al., 1983; Cho and Azam, 1990; Ducklow and Carlson, 1992; Ducklow et al., 1993); and have nutrient uptake potentials around 100 times faster than that of phytoplankton (Blackburn et al., 1998). Studies have shown that bacteria are abundant in the Southern Ocean and are a major pathway for carbon flow despite the low water temperatures and extreme seasonal variation in productivity (Rivkin et al., 1996; Leakey et al., 1996; Delille, 2004).

The viability of bacterioplankton can be greatly affected by viral infection. Virioplankton are important determinants of marine microbial composition and trophodynamics and principal agents of bacterial mortality (Fuhrman, 1999), but little is known of their abundance and role in the Southern Ocean. Their concentrations and virus to bacterial ratios (VBRs), together with the 50–100% loss of bacterial production due to viral infection, indicate they are as important in the Southern Ocean as elsewhere in the world's oceans (Marchant et al., 2000; Guixa-Boixereu et al., 2002).

Despite the vital role of marine microbes in trophodynamics and carbon flux in the Southern Ocean, few studies have determined the abundance and structure of entire microbial communities over large spatial scales in relation to the physical and biotic environment. Other surveys have investigated microbial distribution and abundance off East Antarctica, in the Ross Sea, in the Bransfield Strait, and along transects at 170° W (Smith et al., 2000; Wright and van den Enden, 2000; Waters et al., 2000; Brown et al., 2001; Selph et al., 2001; Vaqué et al., 2002). In our study we used flow cytometry to provide what, to our knowledge, is the largest survey of marine microbes (nanophytoplankton, HNF, bacteria and viruses) in the Southern Ocean and the physical and biotic factors that control them.

2. Methods and materials

The BROKE-West survey covered an area of the Southern Ocean between 30°E and 80°E between January and March 2006 (Fig. 1). The survey consisted of one east-west transect at the northernmost limit of the survey between 60°S and 62°S (leg 12) and 11 meridional transects separated by 5° of longitude and extending from approximately 62°S to the continental shelf. Leg 12 was undertaken first, commencing on 10 January and ending on 19 January 2006. Sampling on the meridional transects commenced in the west (leg 1) on 19 January and ended in the east on 3 March 2007 (leg 11).

Williams et al. (2010) describe the instrumentation used and measurements taken on CTD casts. Briefly, depth profiles were

collected by a suite of sensors measuring fluorescence, conductivity, temperature and dissolved oxygen mounted on a SeaBird 24-bottle rosette frame.

2.1. Flow Cytometry

Seawater for analysis by flow cytometry (FCM) was collected from Niskin bottles (General Oceanics) at four depths over a maximum of 100 m and on every second CTD cast to site 91 on leg 9 (Fig. 1). Sampling ended over the continental shelf on most meridional legs, with the exception of leg 1 where sampling ceased on the continental slope. All samples were analysed fresh using a FACScan (Becton Dickinson) FCM except samples for virus-like particles (VLP) which were preserved and later analysed using a FACScanto FCM (Becton-Dickinson). Both flow cytometers used a 488-nm argon laser. Malfunction of the FCM prevented analysis of fresh samples beyond site 91 on legs 9 and 11. With the exception of virus like particles (VLP), all microbial concentrations are reported as depth integrated concentrations derived using trapezoid and rectangular integration of concentrations to a depth of 100 m.

2.1.1. Nanoplankton

As picoplankton are rare in the Indian Ocean Sector of the Southern Ocean south of 60° S (Kosahi et al., 1985), cells enumerated here are defined as nanoplankton (2–20 µm).

Lysotracker Green-stained HNF (Rose et al., 2004) were discriminated from red autofluorescent nanophytoplankton in bivariate scatter plots of green versus red fluorescence (FL1 and FL3, respectively). As autofluorescent nanophytoplankton in these scatter plots rarely formed discrete clusters, individual populations were not discriminated across the survey area. Subsequently, nanophytoplankton abundances represent a pool of species.

A working solution of Lysotracker Green (Molecular Probes) was prepared daily by diluting the 1 mM commercial stock 1:10 with 0.22-µm-filtered seawater. Ten ml of seawater from each of the four depths at each sample site were stained with 7.5 µl of the working solution (75 nM final concentration) and incubated in the dark and on ice for 10 min. Following incubation, a 1-ml subsample was transferred to a sterile 50 ml Falcon tube and a known concentration of PeakFlow Green 2.5 µm beads (Molecular Probes) was added. Samples were housed in a beaker containing ice and run for 10 min on high flow rate using 0.22-µm-filtered seawater as sheath fluid.

Concentrations of HNF obtained by FCM were compared to those by the standard epifluorescent microscopy method for enumerating heterotrophic protists (Sherr et al., 1993). Briefly, up to 200 ml of 114 samples analysed by FCM were filter-concentrated to 10 ml, stained by 6 drops of 100 mg l⁻¹ 4',6-diamidino-2-phenylindole (DAPI) stock solution for 1 hour in the dark, filtered to dryness and the filter mounted on a glass slide. Cell counts of ≥ 200 cells were obtained from 20 randomly chosen fields of view at x400 magnification using a Zeiss Axioscop equipped for epifluorescence. Ultraviolet excitation was used to detect DAPI-stained cells and blue light excitation was used for chl *a* autofluorescence. Cells of ≤ 20 µm diameter that lacked chl *a* autofluorescence were counted as HNF.

2.1.2. Bacteria

Abundances of total bacteria from fresh samples were determined on all legs with the exception of leg 11 due to malfunction of the FACScan. Total bacterial concentrations in fresh samples were determined by adding a known concentration of Peakflow Green 2.5 µm beads and 2.5 µM final concentration of SYTO13

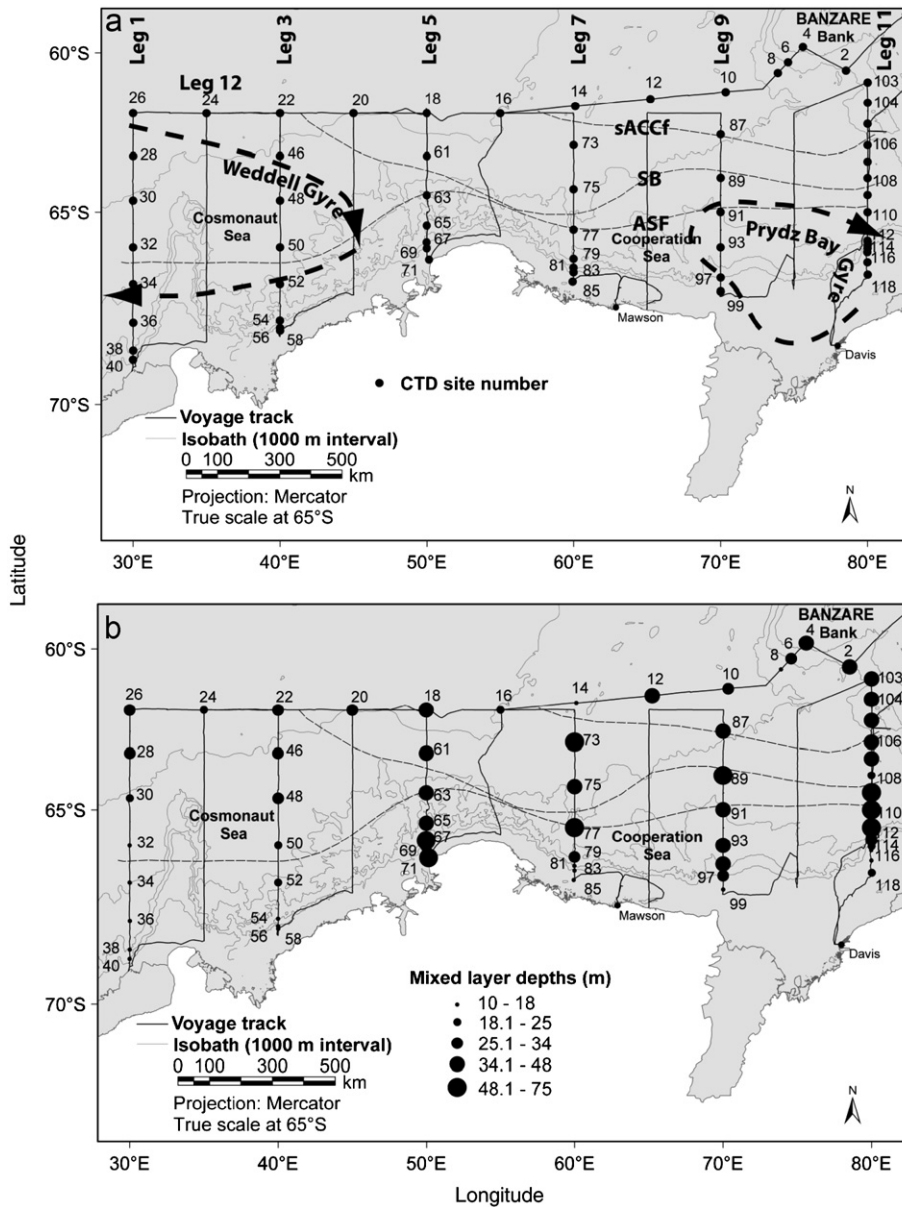


Fig. 1. a) BROKE-West transect legs and numbered CTD sites where samples for FCM were obtained between 30 and 80 °E. Also shown are the locations of the southern Antarctic Circumpolar Current front (sACCF), the Southern Boundary (SB), the northern extent of the Antarctic Slope Front (ASF), the Weddell and Prydz Bay gyres, the Cosmonaut and Cooperation Seas and the BANZARE Bank. b) Summer mixed layer depths over the BROKE-West survey area.

(Molecular Probes) (Gasol and Morán, 1999). Samples were incubated for 20 min in the dark on ice and analysed for 3 mins on low flow rate with MilliQ water as the sheath fluid. Numbers of total bacteria and beads were determined in bivariate plots of side scatter (SSC) versus green fluorescence (FL1) and numbers of microspheres were used to determine the sample volume analysed, allowing the calculation of concentrations of stained bacteria.

Total bacterial concentrations were determined from fixed samples on leg 11. Samples were fixed to a final concentration of 0.5% glutaraldehyde for 20 min before freezing at -80°C for later analysis (Marie et al., 1999). In Australia, samples were rapidly thawed at 37°C , stained for 20 mins using 1:10000 final dilution of SYBR Green I (Molecular Probes) and analysed by FACScan (Marie et al., 1999). Samples were run for 3 min on low flow rate using MilliQ water sheath and were weighed to $\pm 0.0001\text{g}$ before and after each run to determine the volume analysed.

Bacterial numbers were determined from bivariate scatter plots of SSC versus FL1 and the bacterial abundance calculated. Concentrations of bacteria obtained using SYBR Green I may result in overestimates of bacterial concentrations due to increased signal to noise ratios in fixed samples (Lebaron et al., 1998). Thus, concentrations obtained using SYBR Green I are not directly comparable to those obtained from fresh samples using SYTO 13 and should be viewed with caution.

2.1.3. Viruses

VLP were enumerated using a FACScan flow cytometer (Becton-Dickinson). One-ml samples were collected in triplicate from the depth of maximum *in situ* chlorophyll fluorescence determined using the rosette-mounted fluorometer. Samples were fixed with 0.5% (final concentration) of glutaraldehyde in the dark at 0°C for 15 minutes, frozen in liquid nitrogen and

stored at -80°C (Brussaard, 2004). After rapid thawing at 37°C , samples were diluted (1:10) in 0.02 μm filtered TE Buffer (10 mM Tris, 1 mM EDTA, pH 8), stained with SYBR I Green solution (1:5000 dilution) and incubated at 80°C in the dark for 10 minutes (Brussaard, 2004). Acquisition was run for 2 min and 400 to 800 events s^{-1} were collected at $\sim 40 \mu\text{l}^{-1} \text{min}^{-1}$. VLP were discriminated in bivariate plots of FL1 and SSC according to Brussaard (2004). Fluorescent beads of 1 μm diameter (Molecular Probes) were added to all samples, as an internal standard. Stock bead concentrations were estimated after each FCM session under epifluorescent microscopy, to ensure reliability of the beads concentration. Populations of VLP were identified and quantified using WinMDI 2.9 (©Joseph Trotter).

2.2. Statistical analysis

2.2.1. Exploratory Statistics

Microbial concentrations at each site were depth integrated and $\log_{10}(X+1)$ transformed prior to analysis. Cluster analysis was performed using the software package PATN (Belbin, 1993) to determine dissimilarity in community composition and abundance in the survey area. As only total bacterial concentrations were taken on leg 11, these were excluded from the PATN analysis. The Gower metric measure of association was used to generate quantitative estimates of association among sites and these were subjected to flexible hierarchical clustering by unweighted pair-group using arithmetic average (UPGMA) to produce a dendrogram. The mean abundance of microbial groups in each cluster was calculated to characterise the microbial composition of each cluster.

2.2.2. Confirmatory statistics

Microbial distribution and community structure. To determine factors influencing microbial distributions, concentrations of microbes at each sample depth (data not shown) were related to concentrations of chl *a* and the microbial components themselves by Pearson's correlation. Only those that gave significant correlations were further considered. Multivariate analysis of variance (MANOVA) and *post-hoc* Bonferroni tests were used to determine significant differences in microbial abundance amongst the clusters identified by PATN. The paired FCM and epifluorescent microscopy counts were transformed using $\log_{10}(X+1)$ and compared by t-test and simple linear correlation. Statistics were performed using the software package Statistica (v8).

3. Results

3.1. Physical oceanography

The physical oceanography of the survey is detailed by Williams et al. (2010). The Antarctic Circumpolar Current (ACC) formed the northernmost watermass during BROKE-West, flowing eastward but diverging at the BANZARE Bank in the northeast of the survey area (Fig. 1a). The southern Antarctic Circumpolar front (sACCF) in the Circumpolar Deep Water (CDW) of the ACC entered the survey area at approximately 58°E and reached approximately 63°S in the northeast corner of the survey. The Southern Boundary (SB), which defines the southern extent of the CDW and the ACC, entered the survey area at approximately 43°E but reached approximately 65°S at 60°E . The Antarctic Slope Front (ASF) occurred closer to the continent. Two major gyres occurred in the survey area: the eastern extremity of the Weddell Gyre was traversed by legs 1 and 3 in the west and the Prydz Bay Gyre was traversed by legs 7, 9 and 11 in the east.

The BROKE-West survey fell within SIZ and the history of sea-ice cover and retreat strongly influenced the stability and mixed-layer depth of surface waters (Williams et al., 2010). Sea ice retreated from the northeast to the southwest of the survey area between November 2005 and January 2006 but broken sea ice persisted at the southern extent of all legs with the exception of leg 5. Summer mixed-layer (SML) depths reflected the time since retreat of sea ice, being shallow ($< 18 \text{ m}$) at most sites along the coast, increasing to $> 25 \text{ m}$ to the north on legs 1 and 3, and up to 75 m towards the northeast where sea-ice retreat began (Fig. 1b).

3.2. Microbial distribution and abundance

3.2.1. Nanophytoplankton

Nanophytoplankton abundance was generally highest in the south under or near sea ice on legs 1, 3 and 7 where SML depths were shallow. Their abundance was lower in the absence of ice at the base of leg 5 (Fig. 2a). In the Cosmonaut Sea, nanophytoplankton abundance decreased northwards as distance from sea ice increased and the SML deepened. Along the northern extent of the survey (leg 12), concentrations were low in the northeast and northwest but were higher adjacent to, and downstream of, the SB. Nanophytoplankton abundance on legs 1, 3, 7 and 12 was positively correlated with chl *a* concentration (Table 1).

3.2.2. Heterotrophic nanoflagellates (HNF)

The distribution of HNF was similar to and positively correlated with the distribution of nanophytoplankton (Table 1, Fig. 2b). HNF abundance was also positively correlated with chl *a* on all legs except leg 12 where the correlation was significant but negative (Table 1).

Results also suggested interaction between the abundance of HNF and bacteria on some transect legs. On leg 3, HNF abundance was negatively correlated with that of bacteria (Table 2). HNF abundance was moderately high within ice-covered waters (Fig. 2b) while bacterial concentrations were high in ice-free waters (Fig. 2c). In contrast, on leg 5 the abundances of HNF and total bacteria were positively correlated (Table 2). Nanophytoplankton concentrations were moderate on this leg and elevated concentrations of HNF and total bacteria coincided at the northernmost sample site (site 61) and at $\sim 60 \text{ m}$ on site 65, some 30 m below the nanophytoplankton maximum (Fig. 2 a-c, depth data not shown). No significant correlation was found between HNF and total bacteria on other transect legs.

Estimates of HNF concentration obtained by FCM were significantly higher ($\sim 30\%$) than those obtained by microscopy ($t_{0.5,228,2} = -5.951, P < 0.0001$). However, concentrations obtained by both methods were significantly correlated ($r_{(2),0.05, 112} = 0.186, P < 0.001$), indicating that counts by each method resolved different but consistent proportions of the HNF community.

3.2.3. Bacteria

Bacterial abundance was generally highest north of the ASF in the west on legs 3 and 5, reaching $4.76 \times 10^7 \text{ cells cm}^{-2}$ (Fig. 2c). The lowest abundances of $\leq 0.98 \times 10^7 \text{ cells cm}^{-2}$ occurred on legs 7 and 9 within the Cooperation Sea. Moderate to high abundances of bacteria were evident on leg 12 at site 4 over the BANZARE Bank and several sites further west. Abundances on leg 11, obtained using fixed samples stained with SYBR Green I, were very high in the south amongst broken ice cover but decreased northwards in ice-free waters. Bacterial abundance was positively correlated with nanophytoplankton abundance on legs 5, 7 and 12 but was negatively correlated on leg 3.

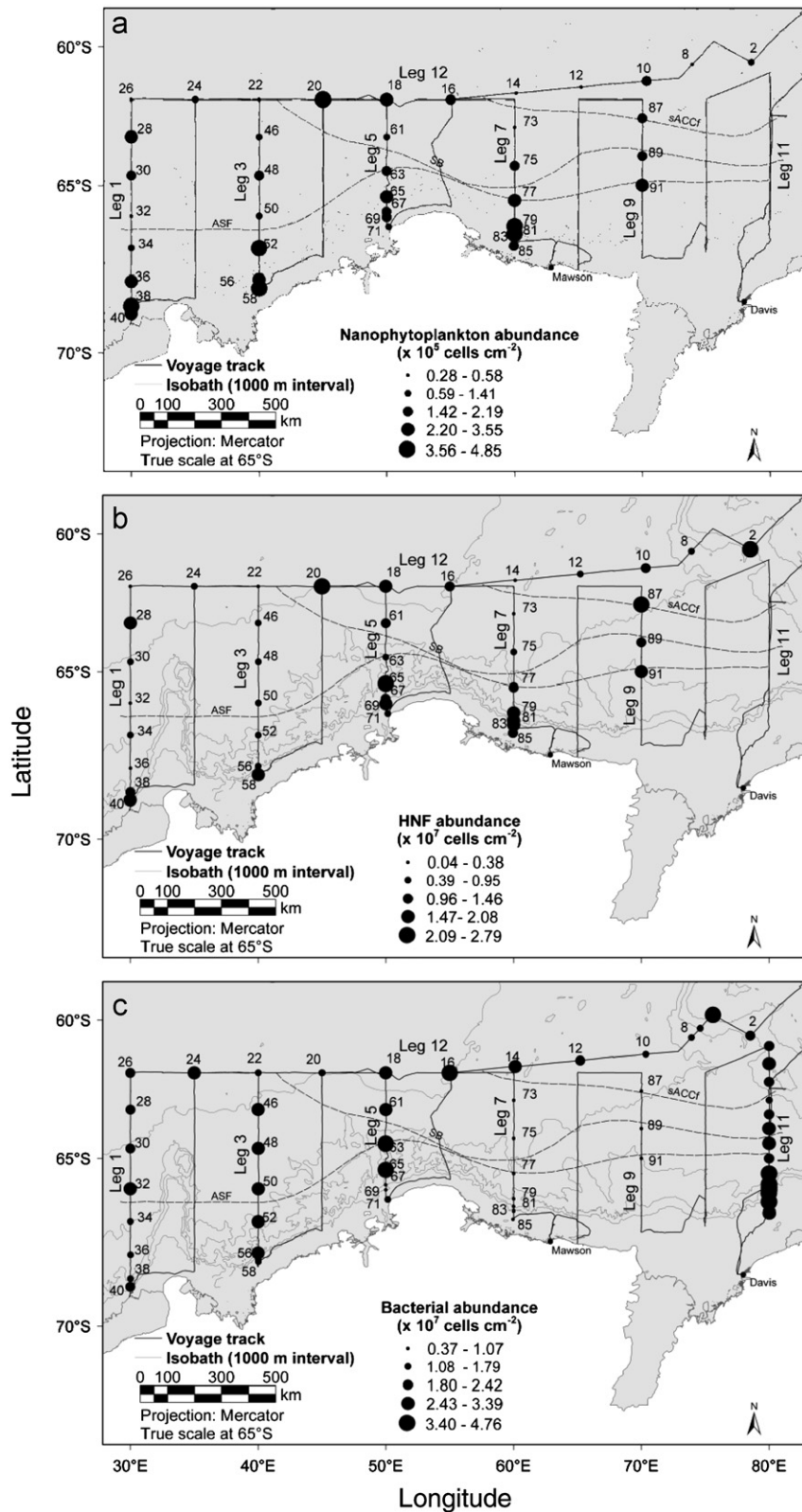


Fig. 2. Distribution and depth integrated abundance of a) nanophytoplankton, b) heterotrophic nanoflagellates (HNF) and c) bacteria over the BROKE-West survey area. Note: bacterial concentrations on transects 1 to 9 were obtained from fresh samples and stained using SYTO 13. On transect 11, concentrations were obtained from fixed samples and stained using SYBR Green. Numbers identify CTD sites.

3.2.4. Viruses

Only one flow cytometric cluster or population of VLP was consistently identified throughout the survey. This cluster was

characterised by low side scatter and SYBR Green fluorescence and was similar to populations observed previously in seawater samples by Marie et al., (1999). This population most likely

Table 1

Significant Pearson correlations for nanophytoplankton and HNF on BROKE-West. Only significant *r* values are shown and marked with probability level (**P* < 0.05, ***P* < 0.01, ****P* < 0.001). Legs are grouped where similar correlations occurred and minimum *r* values shown only. Probability statistic (*r*) for: legs 1, 3 and 7, $r_{0.05(2),73}=0.226$; legs 5 and 9 $r_{0.05(2),44}=0.291$; and leg 12, $r_{0.05(2),28}=0.361$. Note: leg 11 was not sampled for protists.

Biotic factors	Nanophytoplankton – leg #			HNF – leg #		
	1,3,7	5, 9	12	1,3,7	5, 9	12
HNF	0.76***	0.82***	0.77***			
Chl a ($\mu\text{g l}^{-1}$)	0.46***		0.56**	0.34**	0.32*	–0.51**

Table 2

Significant Pearson correlations for total bacteria with biotic factors on BROKE-West. Only significant *r* values are shown and marked with probability level (**P* < 0.05, ***P* < 0.01, ****P* < 0.001). Correlation statistic (*r*) for: leg 1 $r_{0.05(2),25}=0.381$; leg 3 $r_{0.05(2),26}=0.374$; leg 5 $r_{0.05(2),22}=0.404$; leg 7 $r_{0.05(2),26}=0.374$; leg 9 $r_{0.05(2),24}=0.388$; leg 11 $r_{0.05(2),62}=0.246$; and leg 12 $r_{0.05(2),51}=0.273$. Note: leg 11 was sampled only for total bacterial concentrations, na=not available.

Biotic factors	Leg #						
	1	3	5	7	9	11	12
Nanophytoplankton		–0.40*	0.56**	0.52**		na	0.36**
HNF		–0.39*	0.45*			na	

represents bacteriophages as phytoplankton viruses are generally characterised by higher side scatter and/or green fluorescence (Brussaard et al., 1999, 2005, 2008).

The abundance of VLP at each sample site was only determined at the depth of maximum *in situ* chlorophyll fluorescence. VLP abundance reflected the northeast to southwest retreat of sea ice over the survey area (Fig. 3a). The highest concentrations occurred on leg 12 over the BANZARE Bank and west of the SB at site 22 before generally decreasing in concentration towards the base of leg 1. Leg 9 was the exception, having low concentrations and sites that were ice free for long periods. Abundance south of the ASF was high only on leg 5 where sea ice had been absent for up to 83 days (Williams et al., 2010). Virus to bacteria ratios (VBRs, Fig. 3b) were highest on legs 7 and 9 in the Cooperation Sea, reaching 36:1 on these legs and 23:1 in the south of leg 5.

3.3. Cluster groups

Five cluster groups, distinguished at an arbitrary dissimilarity of 0.536, conveniently summarised variation in the composition and abundance of marine microbes during the BROKE-West survey (Fig. 4a,b). The mean microbial abundance of sites in each cluster was calculated to characterise the microbial community. Significant differences among the clusters were determined (Table 3) and the spatial distribution of sites in each cluster was mapped (Fig. 5a,b). The mean abundance of VLP in each cluster varied little (between 1.00×10^6 and $1.45 \times 10^6 \text{ ml}^{-1}$) and did not differ significantly between any of the clusters.

3.3.1. Clusters 1 and 2

Clusters 1 and 2 differed little and were similar in overall community structure (Fig. 4a, Table 3). Cluster 1 mainly contained coastal sea-ice or ice-edge sites between 30° and 70°E (Fig. 5a).

Sites 10 and 20 were the exception, occurring along leg 12 to the north of the sACCF at 70°E and to the east of the SB at 45°E , respectively. Cluster 1 was characterised by high mean depth-integrated concentrations of nanophytoplankton and HNF (3.14×10^5 and $1.51 \times 10^4 \text{ cells cm}^{-2}$, respectively) (Fig. 4a) and low mean concentrations of total bacteria ($1.36 \times 10^7 \text{ cells cm}^{-2}$). However, mean nanophytoplankton abundance varied considerably; 4 sites having $\geq 3.90 \times 10^5 \text{ cells cm}^{-2}$ whilst concentrations at the remaining sites were $\leq 1.66 \times 10^5 \text{ cells cm}^{-2}$.

Most sites in cluster 2 occurred between the ASF and the sACCF in the Cooperation Sea (legs 5, 7 and 9) (Fig. 5a). However, sites 67, 69, 83, and 85 were located amongst the sea ice and/or north of the ice edge. The microbial community consisted of moderate mean concentrations of nanophytoplankton ($2.44 \times 10^5 \text{ cells cm}^{-2}$) but high mean concentrations of HNF ($1.46 \times 10^4 \text{ cells cm}^{-2}$) (Fig. 4). This cluster also had the lowest mean concentration of total bacteria of all clusters ($0.94 \times 10^7 \text{ cells cm}^{-2}$).

3.3.2. Clusters 3 and 4

The overall composition and abundance of the microbial communities in clusters 3 and 4 were strongly dissimilar to and significantly different from clusters 1 and 2, primarily because of the lower abundance of bacteria in clusters 1 and 2 (Table 3a,d, Fig. 4).

Sites in cluster 3 were mainly west of 50°E on legs 1, 3 and 5 in the eastern-most extent of the Weddell Gyre (Figs. 1a, 5b). Five sites were located within the ASF, with 2 sites to its' north on leg 1. Two outlying sites occurred on leg 12 to the east of the SB at 50°E (site 18) and to the northeast of the sACCF near the BANZARE Bank at 75.6°E (site 4). The microbial community in cluster 3 was characterised by the high mean abundance of nanophytoplankton and HNF (3.10×10^5 and $1.35 \times 10^4 \text{ cells cm}^{-2}$ respectively) and high concentrations of bacteria ($2.71 \times 10^7 \text{ cells cm}^{-2}$).

Sites in Cluster 4 also occurred mainly in the west, most being located north of the ASF on legs 3 and 5 in the Cosmonaut Sea (Figs. 1a and 5b). Other sites in this cluster occurred on leg 12 west of the SB at 35°E (site 24), west of the sACCF at 55°E (site 16) and in the northeast near the BANZARE Bank at 78.5°E (site 2). Cluster 4 contained sites with moderate mean concentrations of nanophytoplankton and HNF (1.66×10^5 and $1.11 \times 10^4 \text{ cells cm}^{-2}$, respectively) and the highest concentrations of total bacteria of all clusters ($3.01 \times 10^7 \text{ cells cm}^{-2}$) (Fig. 4b).

3.3.3. Cluster 5

With one exception, sites in cluster 5 occurred on leg 12; the east-west transect of northernmost waters in the survey (Fig. 5b). Most sites in this cluster were located in the ACC but 2 sites fell west of the SB from 40°E . The exception was site 32 that occurred immediately north of the ASF on leg 1.

Bacteria were relatively abundant at sites in cluster 5 but protist concentrations were low. Concentrations of total bacteria reached $2.06 \times 10^7 \text{ cells cm}^{-2}$ while the mean abundance of nanophytoplankton and HNF was lowest of all the clusters (0.41×10^5 and $0.31 \times 10^4 \text{ cells cm}^{-2}$, respectively) (Fig. 4b).

Cluster 5 differed significantly from the coastal and eastern clusters (1 and 2) in overall microbial community composition and abundance (Table 3a) and in each microbial component (Table 3b-d). In contrast, there was no significant overall difference between cluster 5 and the western clusters (3 and 4) (Table 3a). However, cluster 5 had significantly lower concentrations of nanophytoplankton and HNF than cluster 3 and significantly lower concentrations of total bacteria than cluster 4 (Table 3b-d).

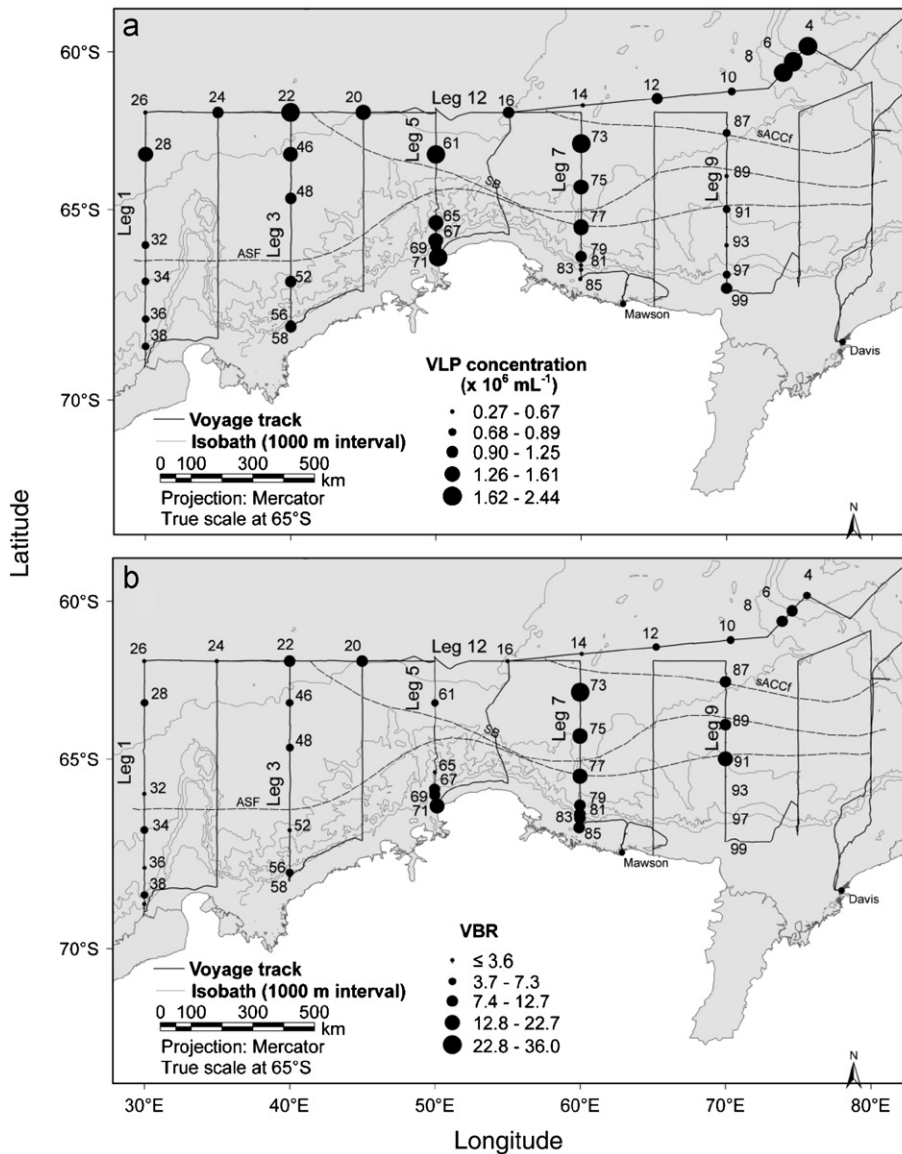


Fig. 3. a) Distribution and abundance of virus like particles (VLP) from the *in situ* chlorophyll fluorescence maximum and b) bacteria to VLP ratios (VBRs) over the BROKE-West survey area. Numbers identify CTD sites.

4. Discussion

The BROKE-West survey offered an unrivalled opportunity to investigate microbial communities over a wide range of environmental variables. This survey was unique, covering approximately 1.5 million km^2 of SIZ, encompassing the continental shelf, several frontal zones, two oceanic gyres, upwelling of MCDW, and areas of the ACC including the shoaling over the BANZARE Bank. Temporally, the survey spanned a period of high microbial productivity (January to March). Thus, the survey encompassed a diverse range of factors influencing microbial distribution, abundance and community composition.

To our knowledge, this is the first study that has used flow cytometry to simultaneously assess synoptic-scale distributions and abundances of auto- and heterotrophic nanoplankton, bacteria and viruses in the Southern Ocean. Selph et al., (2001) and Brown and Landry (2001) used flow cytometry and microscopy to assess protist concentrations between the Antarctic Polar Front and the SIZ at 170°E . However, our study provided a

detailed examination of microbial communities over nearly 40% of the SIZ off East Antarctica.

4.1. Microbial distribution and abundance

4.1.1. Nanophytoplankton

The distribution and abundance of nanophytoplankton was influenced by sea-ice melt and retreat, proximity to the SB, chl *a* and HNF distribution but was also mediated by grazing (Pearce et al., 2010).

In iron sufficient waters surrounding the Antarctic continent, recent disappearance of sea ice releases fresher melt water and creates a shallow mixed layer (Williams et al., 2010). Phytoplankton in these high-light, high-nutrient environments initially escape top-down control by grazers, forming blooms that contribute 25 to 67% of all phytoplankton production in the Southern Ocean (Smetacek et al., 2004; Smith and Lancelot, 2004).

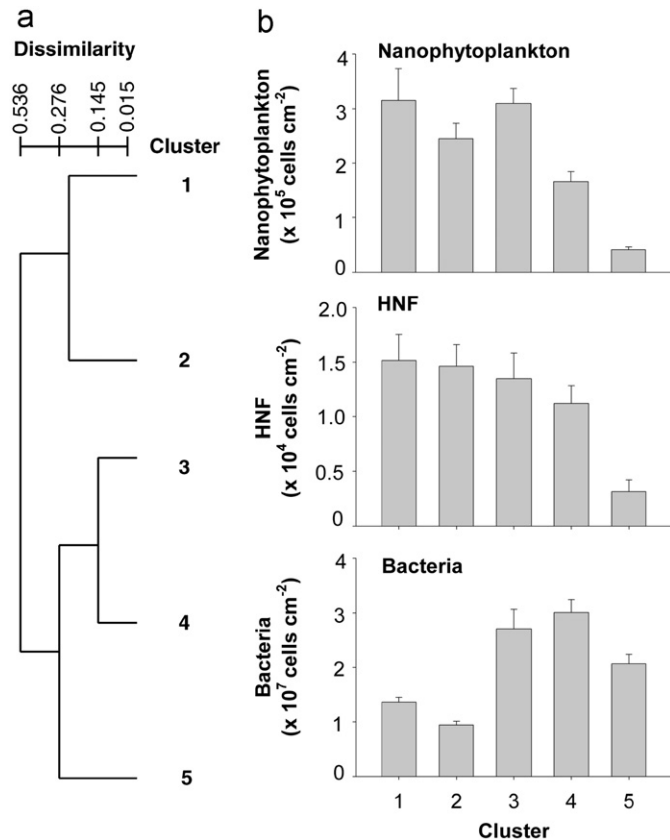


Fig. 4. a) Dendrogram from PATN cluster analysis showing dissimilarity between the 5 clusters and b) mean, depth integrated concentrations of microbes from sites making up the clusters. Error bars denote SE.

Table 3

Probability of significant differences by Bonferroni Test ($\alpha=0.05$) between PATN-defined clusters and their microbial concentrations (Figure 8) in the BROKE WEST survey by a) cluster (df=257); b) nanophytoplankton (nanophyto, df=39); c) HNF, (df=38); and d) total bacteria (df=42). No significant difference where cells are blank.

	Cluster	1	2	3	4	5
a) Cluster	1					
	2					
	3	0.0417	0.0002			
	4	0.0002	< 0.0001			
	5	0.0109	0.0010			
b) Nanophyto	1					
	2					
	3		0.0262			
	4			0.0221		
	5	< 0.0010	0.0490	< 0.0010		
c) HNF	1					
	2					
	3					
	4					
	5	0.0161	0.0090	0.0067		
d) Total bacteria	1					
	2					
	3	0.0003	0.0002			
	4	0.0002	0.0001			
	5	0.0270	0.0002		0.0026	

Nanophytoplankton abundance on BROKE-West declined with increasing distance from sea ice and time since the overall northeast to southwest retreat of ice over the entire survey area,

reflecting the key role of sea ice retreat in fostering nanophytoplankton blooms. The positive correlations between nanophytoplankton and chl *a* concentrations on legs 1, 3 and 7 indicate that nanophytoplankton and larger phytoplankton species were similarly influenced by sea ice melt and retreat. Furthermore, nanophytoplankton were important contributors to the autotrophic biomass on these legs, with nanophytoplanktonic carbon ranging between 38 – 84% of the total autotrophic carbon biomass (Davidson et al., 2010). This range was similar to reports from 13 other Antarctic studies where nanophytoplankton averaged 66% of the total autotrophic biomass (Knox, 2006 and references therein, p.20).

High nanophytoplankton abundances also occurred on leg 12, at sites remote from sea ice but adjacent to the SB. Like Tynan (1998) and Nicol et al. (2000), we conclude that the high abundances at these sites were influenced by upwelling of nutrient rich CDW at the SB.

Nanoplankton taxa identified during BROKE-West are detailed by Davidson et al. (2010). Taxa included chrysophytes (predominately *Parmales* sp.), small diatoms (*Chaetoceros*, *Thalassiosira* and *Fragilariopsis* spp.), dinoflagellates (mostly unidentified gymnodinoids), haptophytes (predominately gametes of *Phaeocystis antarctica*) and prasinophytes (*Pterosperma* spp.).

4.1.2. HNF

We found strong, positive correlations between HNF and nanophytoplankton on all legs. The size spectrum of HNF overlaps that of their prey and they can ingest up to 48% of daily phytoplankton production in the MIZ (Becquevort et al., 1992; 1997; Froneman, 2004). The strong correlation suggests nanophytoplankton were important as prey for HNF and were a primary determinant of HNF abundance across the survey area.

Concentrations of bacteria also appeared to influence HNF abundance. On leg 5, high concentrations of HNF and bacteria co-occurred at sites and depths where nanophytoplankton abundance was low to moderate and where Pearce et al. (2010) found high rates of bacterivory. Thus, the abundance of bacterivorous HNF on this leg appeared to be higher due to the high abundance of their prey. Conversely, the negative correlation between bacterial and HNF abundance on leg 3 may be due to high grazer-induced bacterial mortality (Table 2). HNF identified during BROKE-West by microscopy included choanoflagellates, *Telenema subtile* and other unidentified nanoflagellates (Davidson et al., 2010).

4.1.3. Bacterioplankton

Like HNF, the distribution and abundance of bacteria was also apparently determined by nanophytoplankton. The linkage between phytoplankton and bacterial abundance and productivity in Antarctic waters is controversial. Most authors report a lag between the phytoplankton and bacterial blooms in Antarctic waters, despite reports of correlation between phytoplankton abundance and bacterial activity (e.g. Granéli et al., 2004; Pearce et al., 2007 and references therein). Thus, it is unsurprising that correlations between bacteria and nanophytoplankton abundance were positive (legs 5, 7 and 12), negative (leg 3) or insignificant (legs 1 and 9). Bacterial abundance on legs 3 and 5 increased northwards of sea ice, suggesting herbivory and lysis of senescent phytoplankton blooms increased availability of bacterial substrates. However, this was not true for other legs. The reasons for this are uncertain but may be due to bacterivory (Pearce et al., 2010), viral infection (legs 7), disappearance of phytoplankton blooms due to the prolonged absence of ice (legs 9 and 11), or the absence of blooms at some sites (e.g. along leg 12).

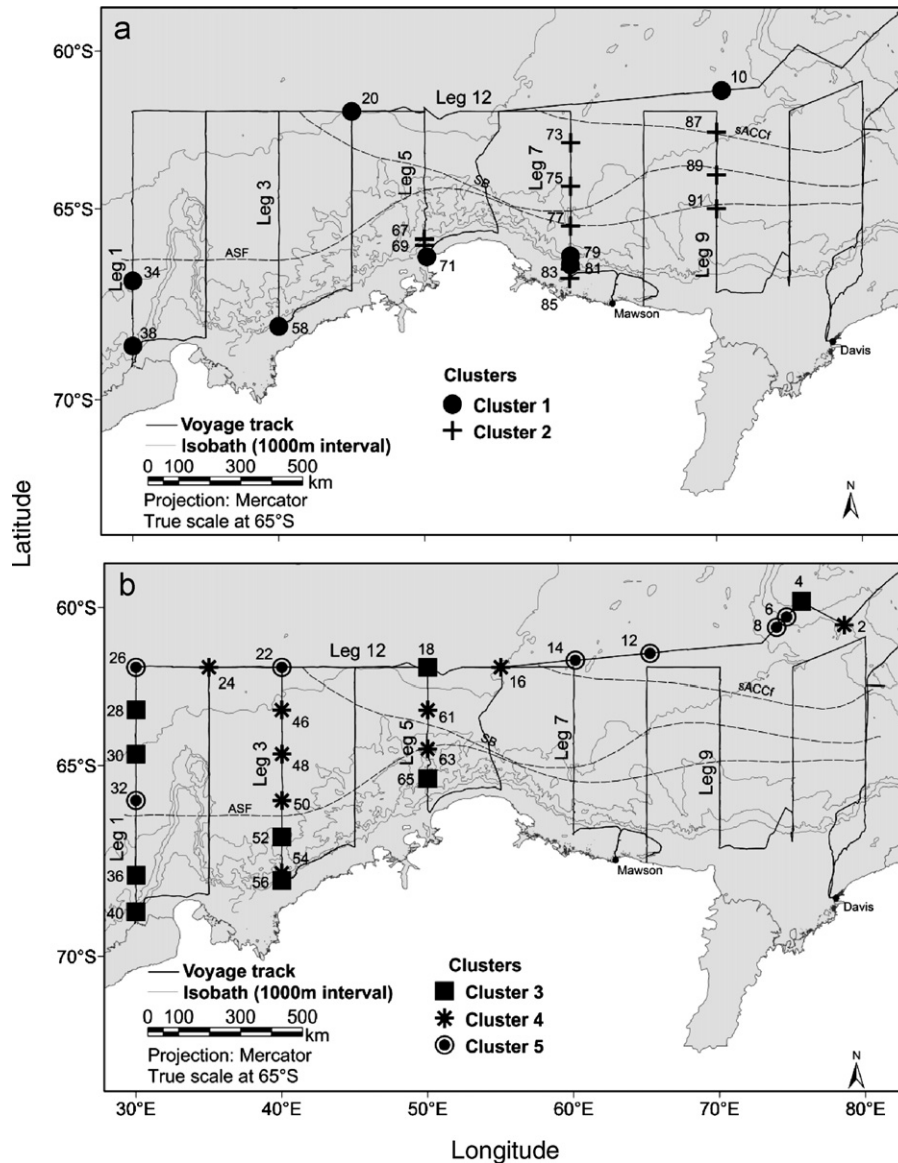


Fig. 5. The distribution of a) bloom type microbial communities from sites in clusters 1 and 2 and b) of senescent (clusters 3 and 4) and POOZ type microbial communities (cluster 5) in the BROKE-West survey region. Numbers identify CTD sites.

4.1.4. Viruses

VLP identified by FCM throughout the BROKE-West survey appeared to be bacteriophages, a finding consistent with assumptions that these represent the bulk of the virus community in most marine habitats (Fuhrman, 1999; Wommack and Colwell, 2000). Other Southern Ocean studies have found that viral abundance increases with primary productivity (Brussaard et al., 2008) and is higher in coastal environments (Guixa-Boixereu et al., 2002). In contrast, on BROKE-West VLP abundance and distribution appeared influenced by the time since sea-ice melt, with the highest concentrations found in the north and/or where sea ice had been absent for long periods and where chl *a* biomass was low. As bacteriophages were dominant during this survey, this pattern may reflect the higher concentrations of bacteria that occur with increasing maturity of microbial communities (see Section 4.3). However, we found no relationship between bacterial and VLP abundance across the BROKE-West survey area, most likely because bacterial maxima over depth (data not shown) rarely coincided with the *in situ* chlorophyll

fluorescence where VLP were sampled. High VBRs were recorded in the Cooperation Sea and are discussed below in section 4.3.2.

4.1.5. Leg 12

Like Pearce et al. (2010), we found that the microbial community on leg 12 was characteristic of high-nutrient low-chlorophyll (HNLC) waters. Unlike other transect legs, the abundance of marine microbes on leg 12 was unrelated to the proximity to sea ice, nanophytoplankton abundance was low, bacterial abundance was moderate and the phytoplankton community was dominated by small flagellate taxa (Pearce et al., 2010). Furthermore, chl *a* concentration was negatively correlated with HNF abundance and the abundances of nanophytoplankton and bacteria were positively correlated. Though within the SIZ, most sites on leg 12 were deeply mixed (Williams et al., 2010) and remote from land. These characteristics are typical of HNLC waters in the POOZ where phytoplankton abundance is limited by iron availability, deep mixing and high

grazing mortality (Becquevort et al., 2000; Smetacek et al., 2004; Smith and Lancelot, 2004) and bacterial production is reportedly closely coupled with phytoplankton-derived substrates (Morán et al., 2004).

4.2. Microbial succession

The relative distribution and abundance of marine microbes is mediated by the successional maturity of the microbial community. Following the initiation of a phytoplankton bloom, succession occurs along a time-line that is reflected in distance from sea ice. The peak or decline of a phytoplankton bloom coincides with maximum heterotrophic biomass and herbivory and low concentrations of bacteria, limited by nutrient availability (e.g. Smith and Lancelot, 2004; Pearce et al., 2008). Grazing and autolysis of phytoplankton releases bioavailable DOC and particulate organic carbon (POC) that are nutritious substrates for bacteria (Jumars et al., 1989; Hygym et al., 1997; Agustí et al., 1998; Nagata et al., 2000; Pearce et al., 2008). As a result, bacterial abundance increases during the decline of phytoplankton blooms and can support extensive bacterivory (e.g. Monticelli et al., 2003; Smith and Lancelot, 2004; Pearce et al., 2008). Senescent blooms are therefore characterised by lower phytoplankton abundance and high heterotroph and bacterial concentrations. Viruses are important agents of bacterial mortality in Antarctic waters (Fuhrman, 1999; Guixa-Boixereu et al., 2002) and are thought to control phytoplankton concentrations and restrict primary productivity (Suttle et al., 1990; Larsen et al., 2001). Virus abundance increases rapidly through cell lysis, thus concentrations of viruses proliferate following the peak and decline of host populations (Larsen et al., 2001).

4.3. Microbial communities

Cluster analysis identified 5 groups of sites that conveniently summarised variation in the microbial community during the BROKE-West survey. Based on microbial correlates and supporting data (Pearce et al., 2010; Westwood et al., 2010; Williams et al., 2010; Wright et al., 2010), these cluster groups represented the HNLC waters on leg 12 and successional stages in the maturity of microbial communities on other legs of the survey.

The high nanophytoplankton and HNF but low bacterial abundance in clusters 1 and 2 indicated these clusters contained sites at which phytoplankton blooms were developing or near their peak.

4.3.1. Cluster 1

The high mean nanophytoplankton abundance indicates that sites in cluster 1 had escaped top-down control prior to sampling. Most sites of this cluster occurred within the sea ice or near the ice edge and nanoplankton were abundant in the shallow SML and bacterial concentrations were low. Supporting data showed that sites in this cluster had rates of primary productivity and concentrations of chl *a* that were the highest for the entire survey (Wright et al., 2010; Westwood et al., 2010). However, rates of microzooplankton grazing were also high (Pearce et al., 2010) suggesting that top-down control of phytoplankton may have begun to limit or reduce phytoplankton abundance by the time the community was sampled. Such communities have previously been described from ice edge blooms in Antarctic waters (Wright and van den Enden, 2000; Selph et al., 2001; Vaqué et al., 2002).

Cluster 1 contained two sites (10 and 20) on leg 12 with bloom communities clearly not derived from stabilisation of the water

column by sea ice retreat. Uniquely for leg 12, the seasonal pycnocline and SML at site 10 shoaled to depths of < 50 m and < 20 m respectively (Williams et al., 2010). Thus, the bloom at this site was probably due to higher light levels in the shallower mixed layer (Nelson and Smith, 1991; Smith et al., 2000). In contrast, the nanophytoplankton bloom at site 20 was probably due to enhancement of primary productivity by upwelling of nutrient rich CDW at the SB (Nicol et al., 2000; Tynan, 1998).

Some sites (10, 34 and 71) had uncharacteristically low concentrations of nanophytoplankton for cluster 1 but moderate to high concentrations of chl *a* (0.92 - 5.99 $\mu\text{g L}^{-1}$) (Wright et al., 2010). Large diatoms and colonies of *Phaeocystis antarctica* were abundant at these sites and nanophytoplanktonic carbon contributed < 19% of the total autotrophic carbon biomass (Davidson et al., 2010). Thus, although nanophytoplankton abundance was low, chl *a* and species concentrations indicate that the identification of these sites as bloom communities in cluster 1 were justified.

4.3.2. Cluster 2

Microbial assemblages at sites in cluster 2 were characterised as blooms constrained by grazing or light availability. Most sites in cluster 2 occurred north of the ASF on legs 7 and 9 in waters of the Cooperation Sea that had been free of ice for > 51 d and had SML depths > 45 m (Williams et al., 2010). Modified Circumpolar Deep Water (MCDW), high in nutrients, shoaled to depths of < 150 m in this region and the Prydz Bay Gyre may have further enriched the area with iron (Westwood et al., 2010; Williams et al., 2010). Thus, blooms at these sites, accompanied by high photosynthetic assimilation numbers (Westwood et al., 2010), appear to be influenced by higher nutrient concentrations. Though not significantly different, nanophytoplankton abundance in cluster 2 was ~ 30% lower than in cluster 1, probably owing to deeper mixing and grazing mortality by abundant HNF, zooplankton and krill at these sites (e.g. Davidson et al., 2010; Jarvis et al., 2010; Pearce et al., 2010; Swadling et al., 2010; Wright et al., 2010).

Other sites in cluster 2 occurred at the ice edge or amongst the broken ice cover on legs 5 and 7 (Wright et al., 2010). Like sites in the area of upwelled MCDW, coastal sites had high nutrient concentrations, high photosynthetic assimilation numbers (Westwood et al., 2010) and occupied an area of the survey where rates of phytoplankton growth and HNF grazing were high (Pearce et al., 2010). Furthermore, the southern extent of leg 5 was ice free for up to 83 days due to the deflection of ice northwards by Capes Anne and Darnley (Williams et al., 2010) and had an SML depth of approximately 40 m. Thus, the similarities in biotic and abiotic factors with the offshore sites support the inclusion of these ice-edge sites in cluster 2.

Mean bacterial concentrations in cluster 2 were the lowest of all clusters. The reasons for this are unclear but coincident data suggests two possible explanations. Rates of bacterivory in the region were variable but commonly high (Pearce et al., 2010) and may have limited their abundance. Alternatively, VLP were abundant on leg 7 and VBRs reached their highest levels of the survey at 36:1. This value is consistent with high infection rates (which typically occur for VBR values > 10), indicating that viral abundance increased following lysis of bacteria (Säwström et al., 2007). Thus, a combination of grazing and viral lysis probably accounted for the low bacterial concentrations recorded in this cluster.

Clusters 1 and 2 in eastern and coastal waters were strongly dissimilar from clusters 3 and 4 in the west, mainly due to consistently higher bacterial concentrations in western clusters.

4.3.3. Cluster 3

Cluster 3 contained sites with high concentrations of nano-phytoplankton, HNF and bacteria, suggesting they were post-bloom communities that were declining due to grazing and senescence. Most sites in this cluster were located west of 50 °E, within the eastern extent of the Weddell Gyre and were characterised by persistent sea ice (leg 1), recent sea-ice retreat or SMLs < 30 m (legs 3 and 5).

The high bacterial concentrations in cluster 3 indicate rapid bacterial growth due to an abundance of bacterial substrate and/or low mortality. This agrees with the findings of Pearce et al. (2010) who reported that rates of herbivory exceeded phytoplankton growth rates in this area while rates of bacterivory were low. Concentrations of DOC were not measured during BROKE-West but senescence of blooms and microheterotroph grazing are known to increase concentrations of DOC, thereby fuelling bacterial growth (Pearce et al., 2007, 2010). Furthermore, pigment data revealed that plumes of senescent microbial matter released from the melting sea occurred at sites 36, 40 and 52 (Wright et al., 2010). Thus, our results indicate that sites in cluster 3 were consistently post-bloom, senescing microbial communities that supported high bacterial abundance.

Post-bloom communities also occurred in the north of the survey and were consistent with ice edge blooms that had senesced during the extended period between the retreat of the ice edge and sampling these sites. Site 4 over the BANZARE Bank was the remnant of a bloom that occurred during December (Schwarz et al., 2010), initiated by upwelling over the shoaling bathymetry of the BANZARE Bank (Sokolov and Rintoul, 2007).

4.3.4. Cluster 4

The microbial community structure of sites in cluster 4 was indicative of mature, post-bloom communities in a senescent phase that was further advanced than seen in cluster 3. Sites in cluster 4 had significantly lower nanophytoplankton abundance than those in cluster 3. Additionally, the carbon:nitrogen ratios at sites in the Cosmonaut Sea were high (Pasquer et al., 2010), indicating advanced remineralisation of POC by bacteria. Like in cluster 3, the location and composition of the microbial community at most sites of cluster 4 were consistent with senescing ice-edge blooms following sea-ice melt and retreat.

Other sites of similar structure occurred over the BANZARE Bank (site 2) and north of the ice edge on leg 3 (site 54) between cluster 3 sites. Site 2 occurred downstream of the BANZARE Bank and, like site 4 in cluster 3, appears to be a senescent population of an earlier bloom. The inclusion of site 54 on leg 3 may reflect the release of senescent material from melting ice (Wright et al., 2010).

Leg 11. Although not included in the cluster analysis due to the absence of data on protist abundance, total bacterial concentrations on leg 11 (80 °E) indicate senescent communities also occurred along this leg. In contrast to other legs, we found very high bacterial concentrations within the broken ice cover, decreasing northwards to the SB. Bacterial abundance on this leg was analysed using fixed samples and SYBR Green and are not directly comparable to those obtained fresh using SYTO 13. However, chl *a* biomass was low (Wright et al., 2010) and satellite observations showed high chlorophyll concentrations occurring approximately 1 month before sampling (Schwarz et al., 2010). Westwood et al. (2010) found low assimilation numbers along the extent of leg 11, indicating phytoplankton cells were in poor health. Furthermore, Pearce et al. (2010) found high concentrations of microzooplankton and high bacterial growth and grazing rates, suggesting a senescent microbial community in the south of this leg. Thus, high bacterial abundances and supporting data

indicate that communities at the southern extent of leg 11 were profoundly senescent.

4.3.5. Cluster 5

Sites in cluster 5, with one exception, occurred on leg 12 and had microbial communities that were typical of HNLC waters in the POOZ, despite being situated within the winter extent of the SZ. Although macronutrients in this cluster were not limiting (Westwood et al., 2010) we found the nanophytoplankton abundance in cluster 5 was lowest of all clusters. Furthermore, Pearce et al. (2010) found that small diatoms, pico- and nanoflagellates dominated the phytoplankton community and their slow growth was matched by rates of microzooplankton grazing. In addition, bacteria abundance was moderately high in cluster 5, suggesting they played a key role in remineralisation and trophodynamics at these sites. The moderately high bacterial concentrations in this cluster were coupled with high rates of bacterial growth and grazing mortality (Pearce et al., 2010). Thus, the bacterial concentrations we observed were probably fuelled by DOC released by microzooplankton grazing. Overall, the balance between production and consumption of phytoplankton and microzooplankton and the high bacterial growth and grazing mortality rates was typical of communities of the HNLC waters of the POOZ.

5. Summary

To our knowledge, this study represents the largest scale survey of microbes undertaken by FCM, providing a comprehensive overview of the physical and biotic controls of microbial community structure and abundance over the BROKE-West survey area. Five distinct microbial communities were identified during the survey. Four reflected different stages in the successional maturity of the microbial community. This maturity increased with distance from the sea ice and, in areas of upwelling, with time since the development of phytoplankton blooms. The fifth occurred at the northernmost extreme of the survey area and were typical of communities in HNLC waters. However, these communities were not spatially contiguous; bloom and post-bloom communities being interspersed on leg 1, due to broken ice cover and the release of senescent sea-ice communities. In the north, HNLC communities were interspersed amongst bloom and senescent communities due to the influence of frontal zones, shallow mixed layers and areas of shoaling bathymetry. Understanding the factors influencing microbial communities will aid in understanding energy flow in the microbial loop, calculating global carbon budgets and predicting the potential ramifications of global climate change on microbial productivity in the Southern Ocean.

Acknowledgments

We thank Captain Scott Laughlin and the crew of the RSV *Aurora Australis* for their dedication and support in supporting the work. We thank staff at Science Technical Support (AAD), in particular Tony Veness and Kelvin Cope for their expertise on the voyage and Bec Gorton, Belinda Ronai, Ben Raymond and David Smith for assistance with programming, data analysis and ArcGIS support. This work was supported by the Australian Government through the Australian Antarctic Division and the Antarctic Climate and Ecosystems Cooperative Research Centre (ACE CRC). We also thank the anonymous reviewers whose suggestions greatly improved the manuscript.

References

- Agustí, S., Satta, M.P., Mura, M.P., Benavent, E., 1998. Dissolved esterase activity as a tracer of phytoplankton lysis: evidence of high phytoplankton lysis rates in the northwest Mediterranean. *Limnology and Oceanography* 43 (8), 1836–1849.
- Azam, F., 1998. Microbial control of oceanic carbon flux: the plot thickens. *Science* 280, 694–696.
- Azam, F., Fenchel, T., Field, J.G., Gray, J.S., Meyer-reil, L.A., Thingstad, F., 1983. The ecological role of water-column microbes in the sea. *Marine Ecology Progress Series* 10, 257–263.
- Azam, F., Smith, D.C., Hollibaugh, J.T., 1991. The role of the microbial loop in Antarctic pelagic ecosystems. *Polar Research* 10, 239–243.
- Beckevort, S., Mathot, S., Lancelot, C., 1992. Interactions in the microbial community of the marginal ice zone of the northwestern Weddell Sea through size distribution analysis. *Polar Biology* 12 (2), 211–218.
- Beckevort, S., 1997. Nanoprotozooplankton in the Atlantic sector of the Southern Ocean during early spring: biomass and feeding activities. *Deep Sea Research II* 44 (1), 355–373.
- Beckevort, S., Menon, P., Lancelot, C., 2000. Differences in the protozoan biomass and grazing during spring and summer in the Indian sector of the Southern Ocean. *Polar Biology* 23, 309–320.
- Belbin, L., 1993. PATN technical reference manual. CSIRO Division of Wildlife and Ecology, Canberra.
- Blackburn, N., Fenchel, T., Mitchel, J., 1998. Microscale nutrient patches in planktonic habitats shown by chemotactic bacteria. *Science* 282, 2254–2256.
- Brown, S.L., Landry, M.R., 2001. Microbial community structure and biomass in surface waters during a Polar Front summer bloom along 170°W. *Deep Sea Research II* 48 (19), 4039–4058.
- Brussaard, C.P.D., Thyrrhaug, R., Marie, D., Bratbak, G., 1999. Flow cytometric analysis of viral infection in two marine phytoplankton species, *Micromonas-pusilla* (Prasinophyceae) and *Phaeocystis pouchetii* (Prymnesiophyceae). *Journal of Phycology* 35, 941–948.
- Brussaard, M., 2004. Optimisation of procedures for counting viruses by flow cytometry. *Applied Environmental Microbiology* 70, 1506–1513.
- Brussaard, C.P.D., Kuipers, B., Veldhuis, M.J.W., 2005. A mesocosm study of *Phaeocystis globosa* population dynamics. I. Regulatory role of viruses in bloom control. *Harmful Algae* 4, 859–874.
- Brussaard, C.P.D., Timmermans, K.R., Uitz, J., Veldhuis, M.J.W., 2008. Virioplankton dynamics and virally induced phytoplankton lysis versus microzooplankton grazing southeast of the Kerguelen (Southern Ocean). *Deep-Sea Research II* 55, 752–765.
- Calbet, A., Landry, M.R., 2004. Phytoplankton growth, microplankton grazing and carbon cycling in marine systems. *Limnology and Oceanography* 49 (1), 51–57.
- Cho, B.C., Azam, F., 1990. Biogeochemical significance of bacterial biomass in the ocean's eutrophic zone. *Marine Ecology Progress Series* 63, 253–259.
- Coffin, R.B., Velinsky, D., Devereux, R., Price, W.A., Cifuentes, L., 1990. Stable carbon isotope analysis of nucleic acids to trace sources of dissolved substrates used by estuarine bacteria. *Applied Environmental Microbiology* 56 (7), 2012–2020.
- Christaki, U., Obernosterer, I., Van Wambeke, F., Veldhuis, M., Garcia, N., Catala, P., 2008. Microbial food web structure in a naturally iron-fertilized area in the Southern Ocean (Kerguelen Plateau). *Deep Sea Research II* 55 (5), 706–719.
- Davidson, A.T., Scott, F.J., Nash, G.V., Wright, S.W., Raymond, B., 2010. Physical and biological control of protistan community composition, distribution and abundance in the seasonal ice zone of the Southern Ocean between 30 and 80°E. *Deep-Sea Research II* 57 (9–10), 828–848.
- Delille, D., 2004. Abundance and function of bacteria in the Southern Ocean. *Cellular and Molecular Biology* 50, 543–551.
- Ducklow, H.W., Carlson, C.A., 1992. Oceanic bacterial production. In: Marshall, K.C. (Ed.), *Advances in Microbial Ecology*. Plenum Press, New York, pp. 113–181.
- Ducklow, H.W., Kirchman, D.L., Quinby, H.L., Carlson, C.A., Dam, H.G., 1993. Stocks and dynamics of bacterioplankton during the spring bloom in the eastern North Atlantic Ocean. *Deep Sea Research II* 40 (1), 245–263.
- Froneman, P.W., Perissinotto, R., 1996. Microzooplankton grazing and protozooplankton community structure in the South Atlantic and in the Atlantic sector of the Southern Ocean. *Deep Sea Research II* 43 (5), 703–721.
- Froneman, P.W., 2004. Protozooplankton community structure and grazing impact in the eastern Atlantic sector of the Southern Ocean in austral summer 1998. *Deep Sea Research II* 51 (22), 2633–2643.
- Fuhrman, J.A., 1999. Marine viruses and their biogeochemical and ecological effects. *Nature* 399, 541–548.
- Garrison, D.L., 1991. An overview of the abundance and role of protozooplankton in Antarctic waters. *Journal of Marine Systems* 2, 317–331.
- Gasol, J.M., Morán, X.A.G., 1999. Effects of filtration on bacterial activity and picoplankton community structure as assessed by flow cytometry. *Aquatic Microbial Ecology* 16, 251–264.
- Granéli, W., Bertilsson, S., Carlsson, P., 2004. Bacterial abundance, production and organic carbon limitation in the Southern Ocean (39–62°S, 4–14°E) during the austral summer 1997/98. *Deep-Sea Research II* 51 (22), 2557–2568.
- Grossmann, S., Dieckmann, G.S., 1994. Bacterial standing stock, activity and carbon production during formation and growth of sea ice in the Weddell Sea, Antarctica. *Applied Environmental Microbiology* 60 (8), 2746–2753.
- Guixa-Boixereu, N., Vaque, D., Gasol, J.M., Sanchez-Camara, J., Pedros-Alio, C., 2002. Viral distribution and activity in Antarctic waters. *Deep Sea Research II* 49 (4), 827–845.
- Hansen, B., Bjørnsen, P.K., Hansen, P.J., 1994. The size ratio between planktonic predators and their prey. *Limnology and Oceanography* 39 (2), 395–403.
- Huntley, M.E., Lopez, M.D.G., Karl, D.M., 1991. Top predators in the southern-ocean – a major leak in the biological carbon pump. *Science* 253, 64–66.
- Hygym, B.H., Peterson, J.W., Sondergaard, M., 1997. Dissolved organic carbon released by zooplankton grazing activity – a high quality substrate pool for bacteria. *Journal of Plankton Research* 19 (1), 97–111.
- Jarvis, T., Kelly, N., Kawaguchi, S., van Wijk, E., Nicol, S., 2010. Acoustic characterization of the broad-scale distribution and abundance of Antarctic krill (*Euphausia superba*) off East Antarctica (30–80°E) in January–March 2006. *Deep-Sea Research II* 57 (9–10), 916–933.
- Jumars, P.A., Penry, D.L., Baross, J.A., Perry, M.J., Frost, B.W., 1989. Closing the microbial loop: dissolved carbon pathway to heterotrophic bacteria from incomplete ingestion, digestion and absorption in animals. *Deep Sea Research II* 36 (4), 483–495.
- Jurgen, K., Wickham, S.A., Rothhaupt, K.O., Santer, B., 1996. Feeding Rates of Macro- and Microzooplankton on Heterotrophic Nanoflagellates. *Limnology and Oceanography* 41 (8), 1833–1839.
- Knox, G.A., 2006. In: *Biology of the Southern Ocean Second Edition* CRC Press, Boca Raton, USA.
- Kosahi, S., Takahashi, M., Yamaguchi, Y., Aruya, Y., 1985. Size characteristics of chlorophyll particles in the Southern Ocean. *Transactions of the Tokyo University of Fisheries* 6, 68–97.
- Larsson, U., Hagström, A., 1982. Fractionated phytoplankton primary production, exudate release and bacterial production in a Baltic eutrophication gradient. *Marine Biology* 67, 57–70.
- Leakey, R.J.G., Archer, S.D., Grey, J., 1996. Microbial Dynamics in coastal waters of east antarctica: bacterial production and nanoflagellate bacterivory. *Marine Ecology Progress Series* 142, 3–17.
- Lebaron, P., Parthuisot, N., Catala, P., 1998. Comparison of blue nucleic acid dyes for Flow Cytometric enumeration of bacteria in aquatic systems. *Applied and Environmental Microbiology* 64 (5), 1725–1730.
- Legendre, L., Ackley, S.F., Dieckmann, G.S., Gulliksen, B., Horner, R., Hoshiai, T., Melnikon, I.A., Reeburgh, W.S., Spindler, M., Sullivan, C.W., 1992. Ecology of sea ice biota. 2. Global significance. *Polar Biology* 12, 429–444.
- Marchant, H., Davidson, A.T., Wright, S.W., Glazebrook, J., 2000. The distribution and abundance of viruses in the Southern Ocean during Spring. *Antarctic Science* 12 (4), 414–417.
- Marie, D., Partensky, F., Vaulot, D., Brussaard, C., 1999. Enumeration of phytoplankton, bacteria, and viruses in marine samples. *Current Protocols in Cytometry Supplement* 10, 11.11.1.
- Mikaloff Fletcher, S.E., Gruber, N., Jacobson, A.R., Doney, S.C., Dutkiewicz, S., Gerber, M., Follows, M., Joos, F., Lindsay, K., Menemenlis, D., Mouchet, A., Müller, S.A., Sarmiento, J.L., 2006. Inverse estimates of anthropogenic CO₂ uptake, transport, and storage by the ocean. *Global Biogeochemical Cycles* 21, GB1010, doi:10.1029/2006GB002751.
- Monticelli, L.S., La Ferla, R., Maimone, G., 2003. Dynamics of bacterioplankton activities after a summer phytoplankton bloom in Terra Nova Bay. *Antarctic Science* 15, 85–93.
- Morán, X.A.G., Gasol, J.M., Pedrós-Alíó, C., Estrada, M., 2004. Dissolved and particulate primary production and bacterial production in offshore Antarctic waters during austral summer: coupled or uncoupled? *Marine Ecology Progress Series* 222, 25–39.
- Nagata, T., Fukuda, H., Fukuda, R., Koike, I., 2000. Bacterioplankton distribution and production in deep pacific waters: large scale geographic variations and possible coupling with sinking particle fluxes. *Limnology and Oceanography* 45 (2), 426–435.
- Nelson, D.M., Smith Jr., W.O., 1991. Sverdrup revisited: critical depths, maximum chlorophyll levels, and the control of southern ocean productivity by the irradiance-mixing regime. *Limnology and Oceanography* 36 (8), 1650–1661.
- Nicol, S., Pauly, T., Bindoff, N.L., Strutton, P.G., 2000. BROKE a biological/oceanographic survey off the coast of East Antarctica (80–150°E) carried out in January–March 1996. *Deep Sea Research II* 47 (12), 2281–2298.
- Pasquer, B., Mongin, M., Johnston, N., Wright, S.W., 2010. Distribution of particulate organic matter (POM) in the Southern Ocean during BROKE-West (30°E–80°E). *Deep-Sea Research II* 57 (9–10), 779–793.
- Paul, J.H., Jeffrey, W.H., DeFlaun, M.F., 1985. Particulate DNA in subtropical oceanic and estuarine planktonic environments. *Marine Biology* 90, 95–101.
- Pearce, I., Davidson, A.T., Bell, E.M., Wright, S.W., 2007. Seasonal changes in the concentration and metabolic activity of bacteria and viruses at an Antarctic coastal site. *Aquatic Microbial Ecology* 47, 11–23.
- Pearce, I., Davidson, A.T., Wright, S.W., van den Enden, R.L., 2008. Seasonal changes in phytoplankton growth and microzooplankton grazing at an Antarctic coastal site. *Aquatic Microbial Ecology* 50, 157–167.
- Pearce, I., Davidson, A.T., Thomson, P.G., Wright, S.W., van den Enden, R., 2010. Marine microbial ecology off East Antarctica (30–80°E): Rates of bacterial and phytoplankton growth and grazing by heterotrophic protists. *Deep-Sea Research II* 57 (9–10), 849–862.
- Pomeroy, L.R., Wiebe, W.J., 1988. Energetics of microbial food webs. *Hydrobiologia* 159, 7–18.

- Rose, J.M., Caron, D.A., Sieracki, M.E., Poulton, N., 2004. Counting heterotrophic nanoplanktonic protists in cultures and aquatic communities by flow cytometry. *Aquatic Microbial Ecology* 34, 263–277.
- Rivkin, R.B., Anderson, M.R., Lajzerowicz, C., 1996. Microbial processes in cold oceans. Relationship between temperature and bacterial growth rate. *Aquatic Microbial Ecology* 10, 243.
- Safi, K.A., Hall, J.A., 1999. Mixotrophic and heterotrophic nanoflagellate grazing in the convergence zone east of New Zealand. *Aquatic Microbial Ecology* 20, 83–93.
- Schwarz, J.N., Raymond, B., Williams, G.D., Pasquer, B., Marsland, S.J., Gorton, R.J., 2010. Biophysical coupling in remotely-sensed wind stress, sea surface temperature, sea ice and chlorophyll concentrations in the South Indian Ocean. *Deep-Sea Research II* 57 (9–10), 701–722.
- Selph, K.E., Landry, M.R., Allen, C.B., Calbet, A., Christensen, S., Bidigare, R.R., 2001. Microbial community composition and growth dynamics in the Antarctic Polar Front and seasonal ice zone during late spring 1997. *Deep Sea Research II* 48 (19), 4059–4080.
- Sherr, E.B., Caron, D.A., Sherr, F.B., 1993. Staining of protists for visualization via epifluorescence microscopy. In: Kemp, P.F., Sherr, B.F., Sherr, E.B., Cole, J.J. (Eds.), *Aquatic Microbial Ecology*. CRC Press, Florida, pp. 213–237.
- Smetacek, V., Assmy, P., Henjes, J., 2004. The role of grazing in structuring Southern Ocean pelagic ecosystems and biogeochemical cycles. *Antarctic Science* 16 (4), 541–558.
- Smith, W.O., Anderson, R.F., Moore, J.K., Codispoti, L.A., Morrison, J.M., 2000. The US southern ocean joint global ocean flux study: an introduction to AESOP. *Deep Sea Research II* 47 (15), 3073–3093.
- Smith, W.O., Lancelot, C., 2004. Bottom up vs top down control in phytoplankton of the Southern Ocean. *Antarctic Science* 16 (4), 531–539.
- Sokolov, S., Rintoul, S.R., 2007. On the relationship between fronts of the Antarctic Circumpolar Current and surface chlorophyll concentrations in the Southern Ocean. *Journal of Geophysical Research* 112, C07030, doi:10.1029/2006JC004072.
- Suttle, C.A., Chan, A.M., Coytrell, M.T., 1990. Infections of phytoplankton by viruses and reduction of primary production. *Nature* 347, 467–469.
- Swadling, K., Kawaguchi, S., Hosie, G.W., 2010. Antarctic mesozooplankton community structure during BROKE-West (30°E–80°E), January–February 2006. *Deep-Sea Research II* 57 (9–10), 887–904.
- Tynan, C.T., 1998. Ecological importance of the Southern Boundary of the Antarctic Circumpolar Current. *Nature* 392, 708–710.
- Vaqué, D., Guixa-Boixereu, N., Gasol, J.M., Pedrós-Alió, C., 2002. Distribution of microbial biomass and importance of protists in regulating prokaryotic assemblages in three areas close to the Antarctic Peninsula in spring and summer 1995/96. *Deep Sea Research II* 49 (4), 847–867.
- Waters, R.L., van den Enden, R.L., Marchant, M.J., 2000. Summer microbial ecology off East Antarctica (80–150°E): protozoan community structure and bacterial abundance. *Deep Sea Research II* 47 (12), 2401–2435.
- Westwood, K.J., Griffiths, F.B., Meiners, K.M., Williams, G.D., 2010. Primary productivity off the Antarctic coast from 30°–80°E; BROKE-West survey, 2006. *Deep-Sea Research II* 57 (9–10), 794–814.
- Williams, G.D., Nicol, S., Aoki, A., Meijers, A.J.M., Bindoff, N.L., Iijima, Y., Marsland, S.J., Klocker, A., 2010. Surface oceanography of BROKE-West, along the Antarctic margin of the south-west Indian Ocean (30–80°E). *Deep-Sea Research II* 57 (9–10), 738–757.
- Wommack, K.E., Colwell, R.R., 2000. Virioplankton: viruses in aquatic systems. *Microbiology and Molecular Biology Reviews*, 69–144.
- Wright, S.W., van den Enden, R.L., 2000. Phytoplankton community structure and stocks in the East Antarctic marginal ice zone (BROKE survey, January–March 1996) determined by CHEMTAX analysis of HPLC pigment signatures. *Deep Sea Research II* 47 (12), 2363–2400.
- Wright, S.W., van den Enden, R., Pearce, I., Davidson, A.T., Scott, F.J., Westwood, K.J., 2010. Phytoplankton community structure and stocks in the Southern Ocean (30–80°E) determined by CHEMTAX analysis of HPLC pigment signatures. *Deep-Sea Research II* 57 (9–10), 758–778.